Korean J. Chem. Eng., **31**(5), 772-779 (2014)
DOI: 10.1007/s11814-013-0255-9

pISSN: 0256-1115
eISSN: 1975-7220

Predicting the velocity distribution of Rushton turbine impeller in mixing of polymeric liquids using fuzzy neural network models

Ali Aminian and Mansour Jahangiri†

Faculty of Chemical, Petroleum and Gas Engineering, Semnan University, P. O. Box 35195-363, Semnan, I. R. Iran
(*Received 4 October 2013 • accepted 26 November 2013*)

Abstract−Velocity profiles are helpful for the confident design of mixing tanks and chemical reactors in mixing processes. A fuzzy model and an artificial neural network have been presented for accurate prediction of velocity distribution of Rushton turbine impeller (RTI) for the mixing of polymeric liquids in the lower transition region: $35<Re'<1800$. Local tangential and radial velocities were predicted along the discharge plane of the impeller. Experimental data were used for training, validation, and testing the neuromorphic models. The presented models are very accurate and reliable in predicting the velocity profiles over wide ranges of polymer concentrations and rotational speed. Comparison of the suggested fuzzy model and the empirical correlations shows that the proposed model outperforms the other alternatives both in accuracy and generality. The results show that the proposed neuromorphic models can successfully be used for prediction of velocity distribution in agitated tanks for viscoelastic polymeric fluids.

Keywords: Fuzzy, Artificial Neural Network, Velocity Distribution, Rushton Turbine Impeller, Polymeric Liquids

INTRODUCTION

Polymer processing in stirred tank reactors has received significant interest in chemical industries. Metzner and Otto (MO) [1-4] proposed that in an agitated vessel, including purely viscous fluids with pseudoplastic properties, an average (effective) shear rate $(dU/dr)_{av}$ could be considered, such that the corresponding apparent viscosity was equal to the viscosity of the Newtonian fluid that would show exactly the same power consumption under identical conditions, at least in the laminar region. They assumed a linear relation between the average shear rate and the rotational speed of the impeller as the following:

$$(dU/dr)_{av}=k_s\cdot N \tag{1}$$

where N is the rotational speed of the impeller in round per second (rps) and k_s is the MO coefficient. However, the significance of the MO method to calculate the effective deformation rate is limited to the laminar flow region and is not valid in the transition region [5-7]. There are, however, some doubts as to whether the MO method is applicable to the transition region [6,8]. Considering many industrial viscoelastic mixing processes with typical Rushton turbine impellers in the transition region, the MO method needs further investigation [9,10].

The fluid motion caused by the rotating Rushton turbine impeller is approximated by an equivalent flow produced in a coaxial cylinder system with the inner cylinder rotating [5]. For a steady and fully developed Couette flow, neglecting the end effects, we can write [11]:

$$\gamma_e=-r\frac{\partial(U/r)}{\partial r} \tag{2}$$

where U is tangential velocity. Therefore, it can be determined the local shear rate using tangential velocity data of this work for different viscoelastic liquid concentrations and impeller speeds. In fact, tangential velocity provides important design information on flow patterns, pumping capacity, power number, mixing time and so on [3,7,8,12].

The Rushton turbine impeller induces a strong radial discharge stream and variations in the radial velocity component with impeller blade angle. Knowledge of flow pattern is very helpful for understanding the impeller performance, i.e., power input, the mixing and circulation times, and the heat transfer rates across the vessel walls [13]. Flow pattern strongly depends on the type and geometry of the impeller [14]. It is difficult to specify an optimal, or sometimes even adequate, agitator configuration for a new application that has unique properties not previously investigated. Experimental evaluation of many different agitator and vessel designs is prohibitively time consuming and expensive. For many industrial materials, such as viscoelastic polymeric liquids, and suspensions, it is impossible or impractical to operate under turbulent mixing. One then has to proceed in the laminar or at best in the transition region. Due to the complexities and uncertainties of mixing in the transition region, it is difficult to predict mixing performance and power requirement for rheologically complex non-Newtonian fluids [15].

The influence of the complex non-Newtonian properties (in particular, viscoelasticity), secondary flow patterns and flow irregularities are expected to be more and more pronounced as the inertial forces become more and more important. This area of research is still in an early exploring stage although some work has been carried out in this field [12,16,17].

Different computational techniques for accurate and low cost design methods have been emphasized for impellers. These methods, such as the finite difference, finite element (based on numerical solution of Navier-Stokes equations, e.g., CFD calculations) [18-24], empirical correlations, non-Newtonian viscosity-shear rate models [25-

†To whom correspondence should be addressed.
E-mail: mjahangiri@semnan.ac.ir

27], and tracer injection techniques [28,29], may be implemented for agitated vessels. However, detailed methods are required to validate the calculations.

A practical correlation for predicting the dimensionless mean radial velocity in the vicinity of impeller tip and on its centerline is as follows [30]:

$$\frac{V}{V_t} = 0.85\left(\frac{r}{R}\right)^{-7/6} \tag{3}$$

A similar correlation to Eq. (3) was derived for dimensionless tangential velocity by introducing a constant related to the velocity profile that depends on the solution properties [20]:

$$\frac{U}{V_t} = 0.85\,\xi_t \exp\left(\frac{r}{R}\right)^{-7/6} \tag{4}$$

Another tangential velocity correlation for different concentrations of PAA solutions and impeller speeds in the lower transition region (i.e., 35<Re′<1800) is [31]

$$\frac{U}{V_t} = m + n\exp\left(\frac{r}{RL}\right)^{-7/6} \tag{5}$$

The validation of CFD as a predictive tool requires comparison of the numerical results and experimental velocity data [20-22]. On the other hand, CFD simulation of applications involving high Reynolds number agitation or multiphase, non-Newtonian solutions can require enormous computational capacity. Laser Doppler velocimetry has proven to be more accurate for the measurement of flow fields in stirred tanks than other techniques such as Pitot probes and hot-wire anemometers because:

(a) It provides flow information even in unsteady and highly turbulent flow regions as well as in the return flow areas of the tank.

(b) It operates without disturbing the flow field [32].

Experimental studies have proved to be successful in measuring the flow field accurately, but they are neither economical nor practical when a large number of the design and process variables is considered. Depending on the purpose of the operation carried out in an agitated tank, the best choice for the geometry of the tank and the impeller type can vary widely. Different materials require different types of impellers and tank geometries to achieve the desired product quality and reasonable operational costs. Other important parameters like impeller clearance from the tank bottom, proximity of the vessel walls, baffle length and number also affect the generated flow.

There are a few studies on the determination of tangential velocity profile for polymeric fluids at discharge plane of Rushton turbine impeller in mixing tanks. Most of them, though, are concerned with measurements of velocity profiles in water representing the agitation of low viscous inelastic fluids.

Thus, there is a lack of experimental data for the velocity profiles of polymeric fluids in mixing processes. Since, performing the mixing experiment for new tanks is costly and time consuming and due to aforementioned shortcomings in empirical and analytical models, it is important to use reliable and accurate tools, which are pertinent to the input-output relations of the concerned system.

The powerful function approximator properties of intelligent techniques make them useful for representing nonlinear and complex models [33,34]. Since evaluation of mixing patterns in stirred tanks and transient mixing phenomena is of great practical interest, a fuzzy model is presented for accurate prediction of tangential velocity in mixing of polymeric viscoelastic liquids.

Furthermore, a three-layered feed forward neural network model has been presented for accurate prediction of radial velocity in mixing of polymeric viscoelastic liquids. In this work, the working fluids were different concentrations of polyacrylamide (PAA) solutions with rheological properties typical of those found in polymeric processes. Also, the effects of concentration of PAA solutions, impeller speeds and radial position on the mixing performance are studied.

EXPERIMENTAL

Measurements were performed in a cylindrical tank of Plexiglas with an inside diameter of 0.276 m and wall thickness of 0.003 m. The tank included four equally spaced baffles of width of 0.03 m. The height of liquid was 0.188 m. The impeller was a typical Rushton turbine with diameter of 0.104 m. The tank and turbine configurations are shown in Fig. 1. The impeller was driven by a variable speed electric motor. The entire tank and motor assembly was mounted on an automated-controlled traversing mechanism, allowing the user to conduct a complete scan of the mixing tank.

The LDA system (Dantec Measurement Technology) was operated in the back scatter mode with both receiving and transmitting optics in the same module. The system consisted of a 5 W Spectra-Physics argon-ion laser, two-color 55x modular optics, two burst spectrum analyzers and a PC. The front focusing lens had a focal length of 0.31 m and produced a beam angle of 9.92°. Additional equipment included an automated three-axis traversing system. The power of the emitted beam (blue-green) could be regulated up to 5 W. This beam was split by a modular optical system into four beams in such a way that two of them were blue rays (488.0 nm) and two others were green (514.5 nm).

Radial and tangential velocities could be obtained simultaneously when the probe traversed along the radius of the mixing vessel. Tan-

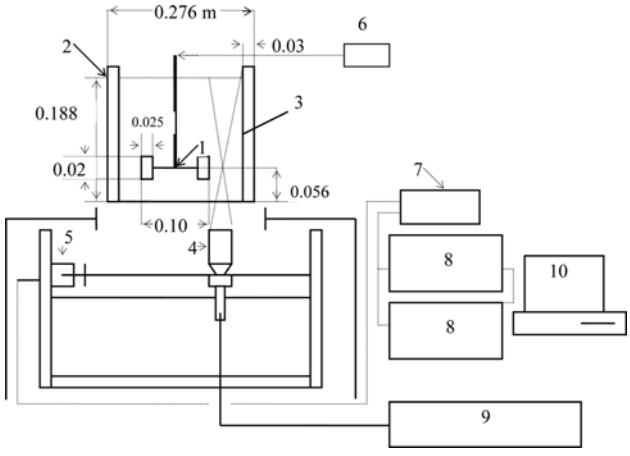

Fig. 1. Setup of LDA and agitated vessel for mixing of polymeric liquids.

1. Impeller
2. Agitated vessel
3. Baffle
4. Laser probe
5. Stepping motor
6. Tachometer
7. Traverse controller
8. Burst spectrum analyzer
9. Laser and its accessory
10. Computer

Table 1. Physical properties of PAA solutions

Fluid	Conc. (ppm)	Density (kg/m^3)	η_0 (kg/ms)
a	500	1114	0.011
b	750	1114.8	0.052
c	900	1120.4	0.0532
d	1350	1128.8	0.139

gential velocities were obtained through the use of green beams and radial velocities by using blues.

Data acquisition and processing of the particle velocity information were done using two Dantec burst spectrum analyzers (BSA). The natural ingredients of PAA solutions were adequate for LDA since for a total of 20k bursts, data rates up to over 1 kHz were easily obtained with more than 60% validity and, therefore, no seeding was required [35]. The total number of collected bursts at each point was such that for any higher number of bursts, only variations less than 0.01 m/s in velocity could be sensed. An oversized filter accepted only the signals from the smallest particles. Calculated average values could be biased in such flows. Continuous-wave mode of measurement took more data from slower-moving particles and in this way reduced the bias error to less than 2 percent [36].

Several concentrations of PAA (Magnofloc LT27 polyacrylamide) solutions in 50/50 (wt%) mixtures of glycerin/water were used as typical viscoelastic polymeric liquids (Table 1). Steady and oscillatory shear experiments were performed by means of a Haake rheometer, RV100/CV100, fully controlled by computer. Rheometric data were measured at the same temperature as that encountered in the mixing experiments.

MODEL DEVELOPMENT

One of the main objectives of polymer engineering research is to increase the predictive capabilities with respect to the effect of process variables. Although it is now recognized that close clearance impellers are more effective for mixing rheologically complex fluids, the classical Rushton turbine remains the most common impeller in industrial and research equipment particularly in the fermentation industry [37]. A fuzzy system is a static nonlinear mapping between its inputs and outputs. The inputs and outputs are crisp, not fuzzy sets. The fuzzification operator converts the crisp inputs to fuzzy sets, the inference mechanism uses the fuzzy rules in the rule-base to produce fuzzy conclusions, and the defuzzification operator converts these fuzzy conclusions into the crisp outputs. This rule base may consist of a series of implications that are defined in the following format, in which the antecedent part is characterized by a logic connective "AND" and the consequence part is represented by a linear equation. In this work, a first-order Takagi-Sugeno fuzzy system was used as estimator. For a first-order Takagi-Sugeno fuzzy model [38], a typical rule set can be expressed as:

If x is A **And** y is B **Then** $f_i=a_{i,0}+a_{i,1}u_1+\ldots+a_{i,n}u_n$ (6)

Where f_i is output from the ith rule and u_j (j=1, 2, …, n) are inputs and $a_{i,j}$ are real fixed numbers referred to as consequent parameters, and x and y are linguistic variables that describe u_j and Y (output from fuzzy system).

For the Takagi-Sugeno fuzzy system, we chose an appropriate operation for representing the premise (e.g., minimum or product), and defuzzification can be obtained using center-average defuzzification

$$Y=\frac{\sum_{i=1}^{Rt} f_i\mu_i}{\sum_{i=1}^{Rt}\mu_i} \tag{7}$$

where Rt is total number of rules and represents the firing strength of each rule defined as premise membership function:

$$\mu_i(u)=\mu_{A_{i1}}(u_1)\times\mu_{A_{i2}}(u_2)\times\cdots\times\mu_{A_{in}}(u_n) \tag{8}$$

where A_{in} are fuzzy sets such as low, medium, high characterized by appropriate membership function, which could be triangular, trapezoidal, Gaussian functions or other shapes. In this study, the Gaussian membership function defined below was utilized:

$$\mu_A(u_j)=\exp\left(-\frac{1}{2}\left(\frac{u_j-c_j}{\sigma_j}\right)^2\right) \tag{9}$$

In consequent part of the rule we use a function $f=g_i(u)$ that is a function of input variables, which in the case of the Takagi-Sugeno fuzzy system can be written as

$$f_i=a_{i,0}+a_{i,1}u_1+\ldots+a_{i,n}u_n \tag{10}$$

Fuzzy systems have very strong interpretability. If properly constructed, they can capture the complex non-linear relationship between inputs and outputs. They are capable of handling complex, nonlinear, and sometimes mathematically intangible dynamic systems. However, when fuzzy rules are extracted by traditional learning methods, there is often a lack of interpretability in the resulting fuzzy rules. Consequently, two common problems are found: the number of rules is usually larger than necessary, and the topology of the fuzzy sets is inappropriate. Therefore, there is always a trade-off between the interpretability and the accuracy of the fuzzy model constructed from sampling data. Recently, attention has been increasingly paid to improve the interpretability of fuzzy systems, and several approaches have been proposed [39-42]. Levenberg-Marquardt learning algorithm, stochastic genetic algorithm, and recursive least square are the main techniques that have received a great deal of attention owing to their fast rate of convergence without extra computations. We applied an efficient approach to construct first-order Takagi-Sugeno fuzzy model from data, considering both their accuracy and interpretability. First, we used the fuzzy C-means clustering method to preprocess the sampling data and to form the rule antecedents of the model. We then used the genetic algorithm (GA) to obtain an initial set of consequent parameters; next, mean least square (MLS) method was used to determine the final rule consequents. This is because GA can reach the region near an optimum point and many function evaluations need to achieve an optimum point. Thus, solution from GA is then used as an initial point for another optimization solver that is faster and more efficient for local search. The number of clusters found by C-means clustering obtained is 15, which are defined by Gaussian membership function for each of the three inputs to build the fuzzy system, which leads to 15 if-then rules containing 90 non-linear parameters and 60 linear parameters (the total parameters is 150) to be learned. We used fuzzy C-means clustering combined with GA and MLS method for training

of a Takagi-Sugeno fuzzy system. The final fuzzy model was obtained in two steps. First, we used the fuzzy C-means clustering method [43,44] to determine the rule antecedents. We then used the GA-MLS method to determine optimal consequent parameters.

Fuzzy clustering can be done using the input-output data, input data only, or output data only. In our approach, we want to use all of the available information. This technique starts to work with an initial guess for the cluster centers. By iteratively updating the cluster centers and the membership grades for each data point, fuzzy C-means iteratively moves the cluster centers to the right location within a data set. This iteration is based on minimizing a cost function that represents the distance from any given data point to a cluster center weighted by that data point's membership grade

$$J=\sum_{k=1}^{M}\sum_{i=1}^{n}\mu_{ik}^{2}(X_k-c_i)^2,\ \sum_{i=1}^{n}\mu_{ik}=1\ \text{ which }\ 1\le k\le M \tag{11}$$

Which must be minimized through a non-linear optimization technique that contains new values of the membership, and the center at each iteration. μ_{ik} is the degree of membership of X_k in the cluster ith.

The experimental data used for developing Takagi-Sugeno fuzzy model are obtained from LDA measurements. The model was trained and tested by using 80% and 20% of a set of 241 velocity points, respectively. Eleven radial positions from the impeller tip to the vessel wall were chosen in order to measure the mean velocity components in mixing of PAA solutions. Local mean velocity and velocity fluctuations at these points were measured for different rotational speeds of the Rushton turbine impeller and various concentrations of PAA solutions. The measured tangential and radial velocities of different PAA concentration were used for training and testing the proposed fuzzy model. The inputs to the fuzzy network are PAA concentration, motor speed (rpm), and the dimensionless radial position, r/R. The PAA concentrations are 500, 750, 900, and 1,350 ppm, the radial position, r/R, spanned between 0.4-0.94 and motor speeds are in the range of 23-100 rpm. The output from the model is tangential velocity normalized by blade tip speed. The input and output data points were normalized, so all data points have the same order of magnitude.

The training performance of the proposed fuzzy model for prediction of tangential velocity according to Gaussian-based MFs is displayed in Fig. 2. As shown, there is a very good agreement between the experimental data and the predicted points. The training phase mean squared error is 4.4×10^{-4}, suggesting the accuracy of the network training. The mean squared error (MSE) is defined as below:

$$MSE=\frac{1}{M}\sum\left(\left(\frac{U}{V_t}\right)^{exp}-\left(\frac{U}{V_t}\right)^{pred}\right)^2 \tag{12}$$

where U is tangential velocity normalized by impeller tip speed V_t and M is total number of data points.

Fig. 3 represents the validation results of the fuzzy model, from which it can be observed that the testing errors for all the testing data set are nearly zero. This clearly indicates the effectiveness and the reliability of the fuzzy model for tangential velocity predictions. The testing phase mean squared error is 1.1×10^{-3}, which indicates the generalizability of the proposed fuzzy model. The fuzzy network modeling and measuring the network performance was implemented under the MATLAB environment.

A similar approach was used to correlate the normalized radial component velocities. In this way a three-layered neural network model was developed for accurate prediction of the radial velocities. A trial-and-error approach was used to minimize the error in order to determine the optimal combination of number of hidden

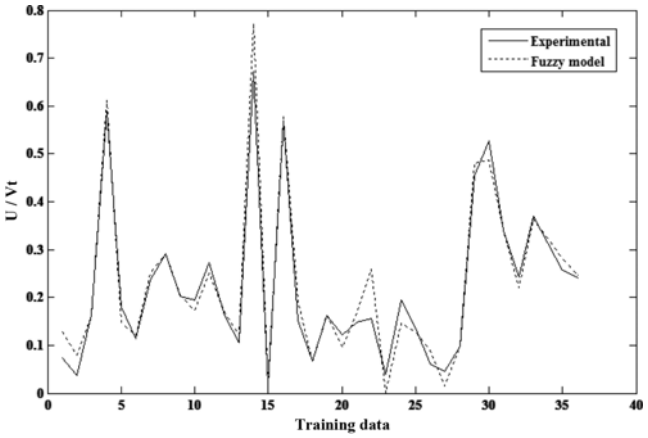

Fig. 3. Fuzzy network testing results for tangential velocity.

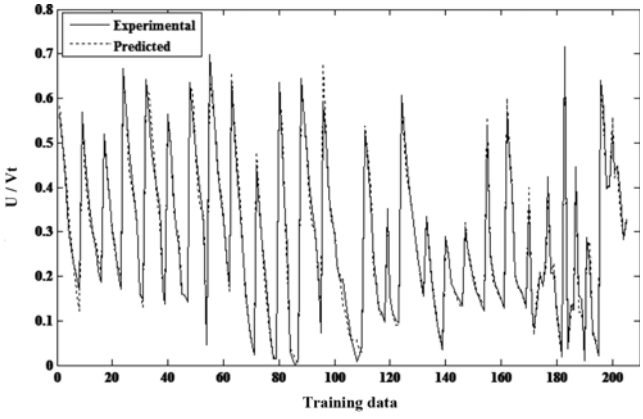

Fig. 2. Fuzzy network training results for tangential velocity.

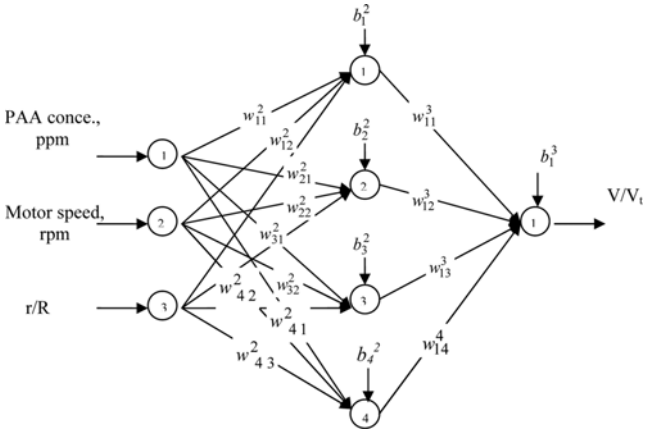

Fig. 4. Neural network architecture.

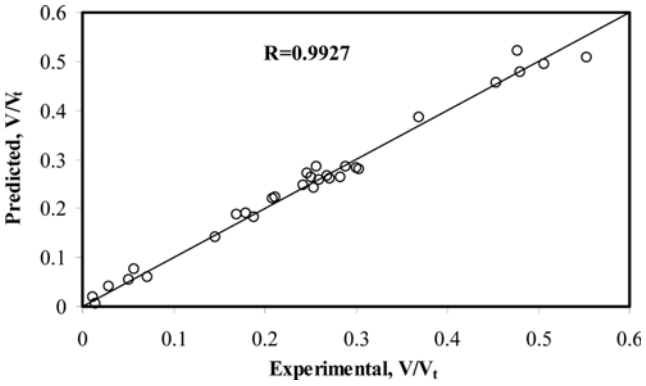

Fig. 5. Comparison between the proposed model predictions with measured normalized radial velocities, training dataset.

Table 2. The optimum values of the three-layered neural network

Hidden layer				Output layer	
Weights			Biases	Weights	Biases
w_{j1}^2	w_{j2}^2	w_{j3}^2	b_j^2	w_{1j}^3	b_1^3
−1.154	−2.302	−0.417	1.147	−0.794	−1.125
0.495	0.529	0.112	−0.306	−2.294	
1.175	0.358	−1.175	1.365	0.515	
0.971	−0.227	−1.813	2.833	0.358	

layers and number of neurons. The best performance is obtained when a network consists of three layers, with three and four neurons in the input layer and the hidden layer, respectively, and one neuron in the output layer is used. The inputs to the neural network model are as before, while the output of the network is normalized radial velocity.

The optimal network architecture for predicting the normalized radial velocity (output of the network) as a function of state variables (input of the network), namely, the PAA concentration (ppm), motor speed (rpm) and radial position is shown in Fig. 4. The training result of the proposed feedforward network is in Fig. 5. As shown, there is a very good agreement between the experimental data and the predicted points. The correlation coefficient (R-value) is 0.9927, very close to 1, suggesting the accuracy of the network training. The optimum calculated values of network parameters to be used in simulations are given in Table 2.

RESULTS AND DISCUSSION

Predicted and measured velocity points are compared with empirical correlations at different radial locations for 1,350 ppm PAA solution in Fig. 6. As shown, the velocity profile reduces exponentially along the radial distance from the impeller. This figure shows that the dimensionless mean tangential velocity for non-Newtonian fluid cannot exceed the impeller speed, $U/V_t<1.0$, and this is contrary to the findings of Stoots and Calabrese [45] for Newtonian liquids.

According to Fig. 6, the effect of radial position on the tangential velocity is more severe in the range of $0.4<r/R<0.6$. That decrease in the tangential velocity occurs almost in this region. After point r/R=0.6, however, this is not the case, due to the presence of the baffle

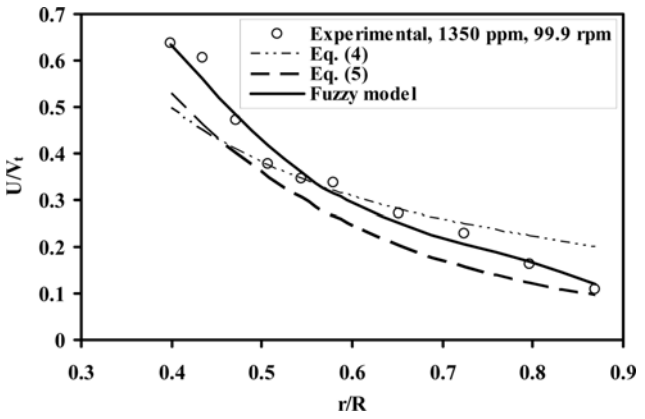

Fig. 6. Comparison of Eqs. (4), (5) and fuzzy model predictions for dimensionless tangential velocities, 1,350 ppm PAA solution, 99.9 rpm.

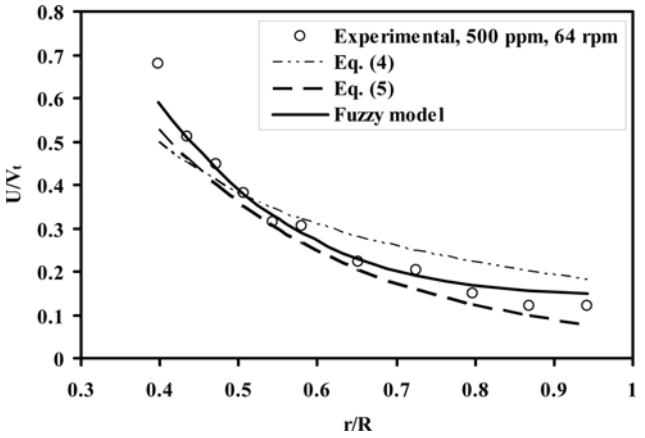

Fig. 7. Comparison of Eqs. (4), (5) and fuzzy model predictions for dimensionless tangential velocities, 500 ppm PAA solution, 64 rpm.

which introduces a relative increase in the turbulence. The proposed fuzzy model outperforms the existing correlations for all radial positions, as shown in Fig. 6.

In Fig. 7 radial profiles of tangential mean velocities on the impeller centerline are presented for 500 ppm PAA solution and at 64 rpm of motor speed. The predicted tangential velocity by newly developed model correlates with the measured data well.

As shown in Figs. 6 and 7, for all PAA concentrations and rotational speeds, Eq. (3) over-predicts the experimental data; while deviation of correlations 4 and 5 from experimental data are lower than Eq. (3). From Figs. 6 and 7 it is clear that Eq. (4) under-predicts the experimental data for distances from r/R=0.4 to 0.6 and over-predicts the experimental data from r/R=0.6 to 0.9. The prediction results of the proposed fuzzy model show good agreement with experimental data for a wide range of operating conditions.

To compare the results of this study and experimental points, variation of tangential velocity against radial position for 900 ppm PAA solution at 44.4 rpm is depicted in Fig. 8. As shown, the velocity is decreased along the radial direction. When the flow reaches the tank wall its velocity decreases rapidly. Near the wall the flow separates into two streams and then it returns back to the impeller region after circulating in the tank. As shown in Fig. 8, it is not possible to cover

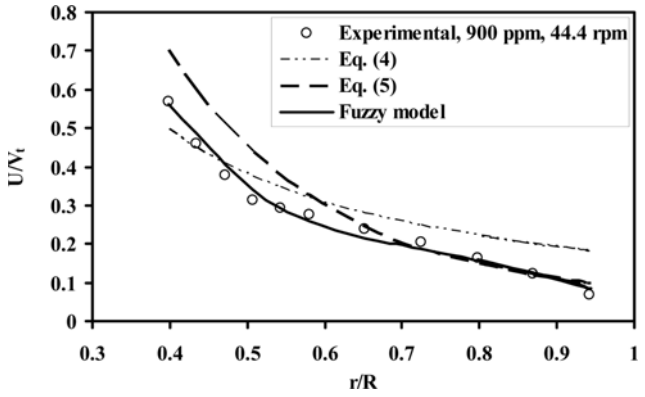

Fig. 8. Comparison of Eqs. (4), (5) and fuzzy model predictions for dimensionless tangential velocities, 900 ppm PAA solution, 44.4 rpm.

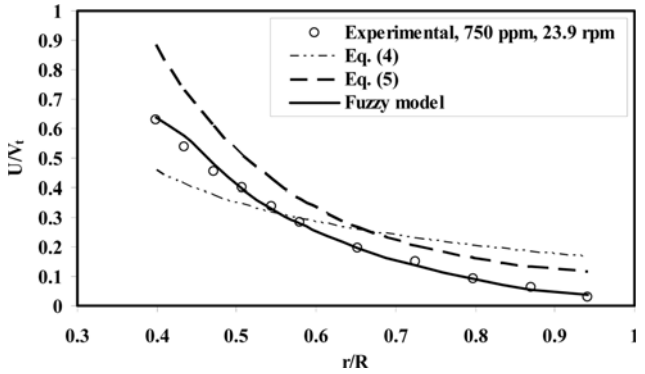

Fig. 9. Comparison of Eqs. (4), (5) and fuzzy model predictions for dimensionless tangential velocities, 750 ppm PAA solution, 23.9 rpm.

all experimental data by the aforementioned correlations. Eq. (5) over-predicts the experimental data until the radial position r/R=0.6; while Eq. (4) over-predicts the velocity points from position r/R=0.5 to 0.9. The predicted tangential velocity points by the proposed fuzzy model are in excellent agreement with measured datasets in all ranges of radial position as shown in this figure.

In the experiments, the impeller clearance from the tank bottom was kept constant at 0.2, so the flow field consisted of smoother circulation when the impeller was placed closer to the tank bottom [46].

Fig. 9 show the velocities in the impeller region obtained via LDA for 750 ppm PAA solution at 23.9 rpm. The normalized tangential velocity profiles in PAA solution are higher than those obtained in Newtonian fluids [16,22].

The presented fuzzy network model accurately predicts the normalized tangential velocities as shown in Fig. 9. The predicted velocity curve (shown as a solid line in Fig. 9) clearly indicates the trend of normalized tangential velocity variations against the radial position.

Fig. 10 shows the comparison between the normalized radial velocity predicted by the proposed three-layered neural network model and experimental measurements vs. radial position for different concentration of PAA solutions and motor speeds. As can be seen from Fig. 10, the profiles of V/V_t data cannot exceed the blade tip speeds. Also, like V/V_t data, the latter result is not similar to the findings of Stoots and Calabrese [45]. Fig. 10 further shows that the region in

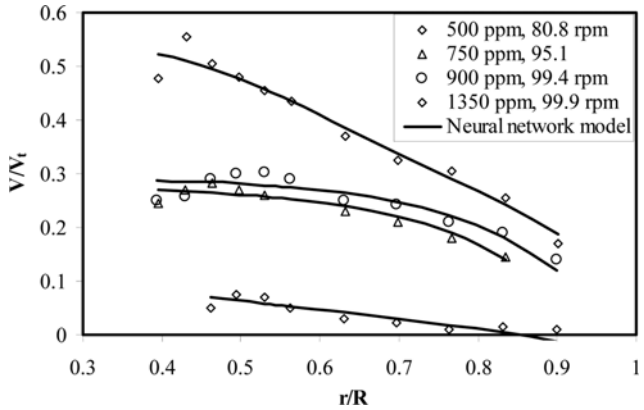

Fig. 10. Comparison of fuzzy model predictions and dimensionless radial velocities.

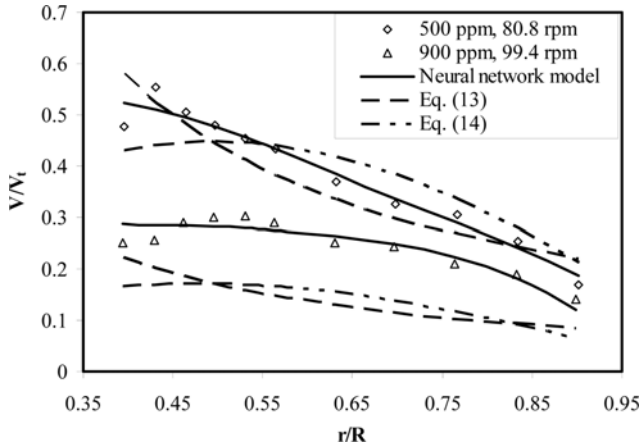

Fig. 11. Comparison of Eqs. (13), (14) and fuzzy model predictions for dimensionless radial velocities, 500 ppm and 900 ppm PAA solutions.

which the profile of V/V_t reaches a maximum, is in the range of $0.4<r/R<0.6$. This behavior may be due to elastic effects in the vicinity of impeller blade such as the Weissenberg effect [11].

For 1,350 ppm solution, at r/R=0.75, the normalized radial velocity approaches zero and this causes the formation of a pseudo-cavern [47]. This phenomenon is a cavern that does not have well-defined boundaries between the stagnant and well-mixed regions. It can be due to the low shear regions formed away from the impeller tip. These results support previous observations by Metzner and Taylor [2] that it is possible to have both laminar and turbulent regimes in an agitated vessel at the same time.

A higher normalized radial velocity is obtained for 500 ppm solution. The peaks in each curve are in the range of $0.4<r/R<0.55$, which do not exist in Newtonian and inelastic non-Newtonian systems.

The predicted velocity points by the proposed neural network model are in excellent agreement with measured radial velocity points in all ranges of PAA concentrations and radial positions as shown in Fig. 10. Furthermore, Fig. 11 compares the result of the three-layered neural network model and empirical correlations for radial velocity,

$$\frac{V}{V_t} = 0.85\,\xi_r\left(\frac{r}{R}\right)^{-7/6} \tag{13}$$

$$\frac{V}{V_t}=\left(a+b\left(\frac{r}{R}\right)\right)\tanh\left(\frac{r}{R}\right) \quad (14)$$

Correlation (13) differs from correlation (3) by introducing a parameter ξ_r, which depends on the Re′. The parameter ξ_r decreases with increasing elasticity of PAA solutions and decreasing of Re′ number and ξ_r for PAA solutions is smaller than those for Newtonian and inelastic non-Newtonian liquids.

As shown in Fig. 11, for 900 ppm solution, both correlations (13) and (14) under-predict the experimental data significantly. For 500 ppm solution, it is not possible to cover all experimental data by the aforementioned correlations.

Predicted radial velocities are compared with the set of experimental data points, which are not used in the model development in Fig. 12. The overall correlation coefficient (R-value) of 0.9919 indicates a very good agreement between experimental and predicted radial velocities.

The generalizability of the models is shown in Figs. 3 and 12. The predicted velocities for the datasets that were not used in the training phase (unseen to the models) indicate a very good agreement between experimental and predicted velocities for testing datasets. Effect of PAA concentration on normalized radial velocity is more important at high radial positions, as shown in Fig. 13. At a low radial position of r/R=0.5, a decrease of PAA concentration from 1,350 to 500 ppm leads to an increase in radial velocity from 0.072 to 0.465, while at a higher radial position of r/R=0.9, the same PAA increment results in a considerable increase in radial velocity from 0.009 to 0.17. For wide ranges of PAA concentrations and radial positions, the presented neural network model accurately predicts the normalized radial velocities as shown in Fig. 13.

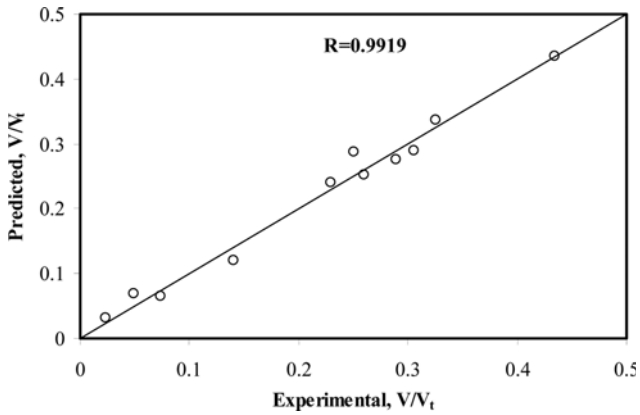

Fig. 12. Comparison between the proposed model predictions for measured normalized radial velocities, testing dataset.

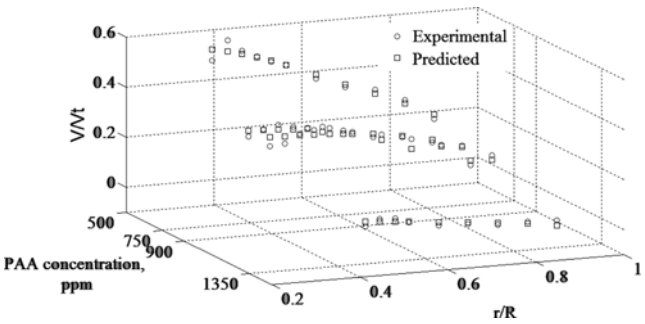

Fig. 13. Comparison of the predicted normalized radial velocity for experimental data.

CONCLUSIONS

Accurate prediction of tangential and radial velocities for viscoelastic polyacrylamide (PAA) solutions through LDA velocity measurements with a typical Rushton turbine has been presented in the lower transition region: 35<Re′<1800.

A fuzzy model and three-layer feedforward artificial neural network with four neurons in the hidden layer and one neuron in the output layer has been presented for predicting the normalized tangential and radial velocities in stirred tank reactors, respectively. The fuzzy model was used for predicting the tangential velocity, while the three-layer feedforward artificial neural network model was used for predicting the radial velocity. Fuzzy C-means has been applied for data clustering in the fuzzy model to obtain the antecedent parameters, and least square method was used for optimizing the consequent parameters. The three-layer neural network was trained by using the Levenberg-Marquardt back propagation algorithm and the tan-sigmoid activation function was applied to calculate the output values of the neurons of the hidden layer. The presented models are very accurate and reliable for predicting the tangential and radial velocities for viscoelastic polymeric solutions over wide ranges of polymer concentrations and radial positions. At radial positions above 0.7, an increase in PAA concentration leads to a significant decrease in radial velocity. The effect of radial position on tangential velocity is much more important at 0.4<r/R<0.6. The presented models outperform the other available correlations regarding the prediction of tangential and radial velocities. The predicted tangential and radial velocities can be used to calculate local shear rates and power consumption of the mixer as well as knowledge of mixing intensity in the mixing tank. The predicted velocities are in excellent agreement with experimental data, suggesting the accuracy of the proposed models for proper design of stirred tanks in mixing processes.

NOMENCLATURE

a, b : constants defined in Eq. (14)
$a_{i,j}$: consequent parameter for j-th input and i-th rule
A_{in} : fuzzy sets
b_j : bias value of the j-th neuron
c : center value
D : impeller diameter, m
exp : experimental
f_i : output from the i-th rule
i : i-th input
J : objective function
k : data-pair index
M : number of datapoints
MSE : mean square error
n : number of inputs
N : rotational speed, rev/s, rpm
pred : predicted
r : radial coordinate [m]
R : radius of agitated vessel [m]

Rt : total number of rules
Re′ : zero shear rate Reynolds number=$\rho ND^2/\eta_0$
u_j : j-th input to the fuzzy system
U : tangential velocity [m/s]
V : radial velocity [m/s]
V_t : impeller tip speed, πDN [m/s]
w_{ji} : weight value between i-th input and j-th neuron of the input and hidden layers
w_{kj} : weight value between j-th hidden neuron and the k-th neuron of the output layer
x : input linguistic variable
X : input-output data pairs
y : output linguistic variable
Y : fuzzy system output

Greek Letters

ξ_r : van der Molen and van Maanens correlating constant for radial velocity
ξ_t : van der Molen and van Maanens correlating constant for tangential velocity
μ_i : fire-strength of i-th rule
$\mu_{A_{in}}$: membership function of the i-th rule and for each fuzzy set
μ_{ik} : membership function defined in Eq. (11)
σ : width value
η_0 : zero shear rate viscosity [kg/ms]
μ : Newtonian viscosity [kg/ms]
ρ : density [kg/m^3]

REFERENCES

1. A. B Metzner and R. E. Otto, *AIChE J.*, **3**, 3 (1957).
2. A. B Metzner and J. S. Taylor, *AIChE J.*, **6**, 109 (1960).
3. D. Doraiswamy, R. K. Grenville and A. W. Etchells, *Ind. Eng. Chem. Res.*, **33**, 2253 (1994).
4. Z. Minge, Z. Lühong, J. Bin, Y. Yuguo and L. Xingang, *Chinese J. Chem. Eng.*, **16**, 686 (2008).
5. S. Foucault, A. Gabriel and P. A. Tanguy, *Ind. Eng. Chem. Res.*, **44**, 5036 (2005).
6. P. J. Carreau, R. P. Chhabra and J. Cheng, *AIChE J.*, **39**, 1421 (1993).
7. P. Forschner, R. Krebs and T. Schneider, in *Scale-up procedures for power consumption of mixing in non-Newtonian fluids*, Proc 7th Euro Conf on Mixing, Brugge, Belgium, 161 (1991).
8. J. J. Ulbrecht and P. J. Carreau, in *Mixing of viscous non-Newtonian liquids in mixing of liquids by mechanical agitation*, J. J. Ulbrecht and G. K. Patterson Eds., Gordon and Breach Science, NewYork (1985).
9. M. Jahangiri, M. R. Golkar-Narenji, N. Montazerin and S. Savarmand, *Chinese J. Chem. Eng.*, **9**, 77 (2001).
10. M. Jahangiri, *Iran. Polym. J.*, **17**, 831 (2008).
11. R. B. Bird, R. C. Armstrong and O. Hassager, *Dynamics of polymeric liquids*, Fluid Mechanics, 2nd Ed., John Wiley, New York, 1 (1987).
12. J. Cheng and P. J. Carreau, *Can. J. Chem. Eng.*, **72**, 418 (1994).
13. R. Escudie, D. Bouyer and A. Line, *AIChE J.*, **50**, 86 (2004).
14. D. M. Mad, L. F. Feng, K. Wang and Y. L. Li, *Can. J. Chem. Eng.*, **75**, 307 (1997).
15. J. M. Smith, *Trans. Inst. Chem. Eng.*, **68**, 3 (1990).
16. P. M. Armenante, C. Luo, C. C. Chou, I. Fort and J. Medek, *Chem. Eng. Sci.*, **52**, 3483 (1997).
17. J. Pérez-Terrazas, V. Ibarra-Junquera and H. Rosu, *Korean J. Chem. Eng.*, **25**, 461 (2008).
18. R. Zadghaffari, J. S. Moghaddas and J. Revstedt, *Comput. Chem. Eng.*, **33**, 1240 (2009).
19. M. Rahimi, A. Kakekhani and A. Alsairafi, *Korean J. Chem. Eng.*, **27**, 1150 (2010).
20. E. Koutsakos, A. W. Nienow, K. N. Dyster, fluid mixing IV, *IChemE Symp.* Bradford, UK, **121**, 51 (1990).
21. B. H. Um and T. Hanley, *Korean J. Chem. Eng.*, **25**, 1094 (2008).
22. K. Yapici, B. Karasozen, M. Schafer and Y. Uludag, *Chem. Eng. Process.*, **47**, 1340 (2008).
23. F. G. Smith, *Chem. Eng. Sci.*, **52**, 1459 (1997).
24. J. C. Middleton, F. Pierce and P. M. Lynch, *Chem. Eng. Res. Des.*, **64**, 18 (1986).
25. G. Couerbe, D. F. Fletcher, C. Xuereb and M. Poux, *Chem. Eng. Res. Des.*, **86**, 545 (2008).
26. T. C. Papanastasiou and A. G. Boudouvis, *Comp. Struct.*, **64**, 677 (1997).
27. V. V. Ranade, *Chem. Eng. Sci.*, **52**, 4473 (1997).
28. J. Behin and S. Bahrami, *Chem. Eng. Process.*, **59**, 1 (2012).
29. D. Lelinski, J. Allen, L. Redden and A. Weber, *Miner. Eng.*, **15**, 499 (2002).
30. K. Van der Molen and H. R. E. Van Maanen, *Chem. Eng. Sci.*, **33**, 1161 (1978).
31. M. Jahangiri, *Iran. Polym. J.*, **14**, 521 (2005).
32. M. Schaefer, M. Hufken and F. Durst, *Trans. IChemE.*, **75**, 729 (1997).
33. B. ZareNezhad and A. Aminian, *Korean J. Chem. Eng.*, **28**, 1286 (2011).
34. A. Aminian, *Chem. Eng. J.*, **162**, 552 (2010).
35. N. Montazerin, A. Damangir and S. Mirian, in *A new concept for squirrel-cage fan inlet, Proc. Instn. Mech. Eng.*, **212**, 343 (1998).
36. D. A. Johnson, D. Modarress and F. K. Owen, *Trans. ASME J. Fluids Eng.*, **106**, 5 (1984).
37. T. Espinosa-Solares, E. Brito-De la Fuente, A. Tecante and P. A. Tanguy, *Chem. Eng. J.*, **67**, 215 (1997).
38. T. Takagi and M. Sugeno, *IEEE Trans. Sys. Man. Cybern.*, **15**, 116 (1985).
39. H. Wang, S. Kwonga, Y. Jinb, W. Wei and K. F. Man, *Fuzzy Sets. Sys.*, **149**, 149 (2005).
40. Y. Jin, W. V. Seelen and B. Sendhoff, in *An approach to rule-based knowledge extraction, Proc. IEEE Conf. Fuzzy Sys.*, **2**, 1188 (1998).
41. I. Rojas, H. Pomares, J. Ortega and A. Prieto, *Trans. Man. Cybern.*, **8**, 23 (2000).
42. H. Roubos and M. Setnes, *Trans. Fuzzy Sys.*, **9**, 516 (2001).
43. J. C. Bezdek, *Pattern recognition with fuzzy logic objective function algorithm*, Plenum Press, New York (1981).
44. K. M. Passino, *Biomimicry for optimization, control and automation*, Springer-Verlag, London (2005).
45. C. M. Stoots and R. V. Calabrese, *AIChE J.*, **41**, 1 (1995).
46. P. V. Bartels, *An experimental study on turbulent mixing of viscoelastic fluids*, Ph.D. Thesis, University of Delft (1988).
47. Y. Hirata, A. W. Nienow and I. P. T. Moore, *J. Chem. Eng. Japan*, **27**, 235 (1994).